

### The effects of shear and co-surfactants on the evolution of the micro-structure in concentrated di-chain cationic surfactant solutions

J. Penfold<sup>1</sup>, E. Staples<sup>1</sup>, I. Tucker<sup>2</sup>, J. Hubbard<sup>2</sup>, L. Soubiran<sup>2</sup> & A. Creeth<sup>2</sup>

[1] ISIS Facility, CLRC, Rutherford Appleton Laboratory, Chilton, Didcot, Oxon.

[2] Unilever Research, Port Sunlight Laboratory, Quarry Road East, Bebington, Wirral.

*Fibre Diffraction Review* **11**, 68-74, 2003

#### ABSTRACT

*We have previously reported the use of small-angle neutron scattering, SANS, rheology, and conductivity to characterise the shear thickening transition from an aligned lamellar phase to liposomes [1]. The SANS and conductivity measurements indicate an inhomogeneous distribution of order across the Couette flow cell gap. We present Small-Angle X-ray Scattering, SAXS, data using a micro-focus X-ray beam, which demonstrates the same inhomogeneity. Polarised light scattering measurements in the region of the shear thickening transition show a marked increase in texture. Both measurements provide evidence which is consistent with common stress and common strain 'banding' [2].*

*Preliminary results on the effects of temperature and the addition of co-surfactants are discussed. Both the addition of co-surfactant and the temperature relative to the  $L_\alpha/L_\beta$  transition temperature are shown to have a profound effect on the solution micro-structure. For solutions which are a mixture of the di-chain cationic and a non-ionic surfactant, rich in the di-chain cationic surfactant, increasing temperature results in a more ordered lamellar structure. For solutions richer in the non-ionic co-surfactant, increasing temperature induces the formation of mixed micelles.*

#### Introduction

Shear induced transitions in surfactant systems have been extensively studied and reported; and include isotropic to nematic transitions [3], growth of elongated micelles [4], lamellar to vesicle transitions [1,5], and variations in orientational order in lamellar phase systems [6,7]. More specifically we have recently reported the characterisation of the shear-thickening transition from an aligned lamellar phase to multi-lamellar vesicles in the di-chain cationic surfactant system, di-octadecyl dimethyl ammonium chloride, 2HT [1]. We compared the behaviour of this charge-stabilised system under shear with those stabilised by ' Helfrich fluctuations' [5]. Such fluctuations are stabilised by a long range repulsive force arising from thermal fluctuations in the lamellar bi-layer. As part of that study, the SANS and conductivity data gave results that were indicative of an inhomogeneous distribution of orientational order across the Couette flow cell gap. It is this aspect that will be pursued in more detail in the first part of the present paper. We have

previously shown, in a different lamellar phase system, that changes in orientational order in lamellar phase dispersions are observed as a function of shear [6,7]. In related studies, Berghausen *et al.* [8] have shown that this can be associated with changes in distribution across the Couette flow cell gap in the shear gradient direction.

The original SANS and conductivity data [1] indicate an inhomogeneous distribution of order for the 2HT dispersions, and further SANS data and SAXS data, using a micro-focus beam-line, were used to investigate the distribution in orientational order. Shear-induced phase separation has been the subject of much recent theoretical interest [2,9,10]. Shear-induced phase separation, or 'shear banding', associated with a discontinuity in the stress-strain relationship, is predicted for common stress (in the shear gradient direction), and for common strain (in the vorticity direction). This has now been well-established for a variety of different systems, and we discuss our data in the context of 'shear banding'.

Temperature and the addition of a co-surfactant can both have a profound effect on the macroscopic behaviour and on the micro-structure of lamellar phase dispersions. In many practical applications and formulations non-ionic surfactants are used to manipulate (reduce) the dispersion viscosity. Reductions in lamellar fragment size, where the non-ionic surfactant adsorbs to the fragment edge hence stabilising smaller fragments, are observed [11]. Temperature is also important, as the temperature relative to the  $L_\alpha / L_\beta$  transition temperature dictates its macroscopic behaviour and its micro-structure. In the second part of the paper we report preliminary results on the effects of co-surfactant and temperature on the dispersion micro-structure.

## Experimental Details

The SANS measurements were made on the LOQ diffractometer at ISIS [12], using the white beam time-of-flight method, in the scattering vector,  $Q$ , range of 0.008 to 0.25  $\text{\AA}^{-1}$ . A quartz Couette flow cell, described previously by Penfold *et al.* [13]; with a 50 mm diameter, a 0.5 mm gap, a fixed inner stator, and a rotating outer cup was used. Measurements were made for shear rates from 0 to 1000  $\text{s}^{-1}$ , and for temperatures in the range 25 to 60  $^\circ\text{C}$ . The SAXS measurements were made on the ID13 X-ray micro-focus beam-line at the ESRF [14]. SAXS data were recorded using a 20 x 20 micron beam at a wavelength of 0.96  $\text{\AA}$ , in the  $Q$  range 0.002 to 0.3  $\text{\AA}^{-1}$ . A poly-carbonate Couette flow cell with an outer diameter of 20 mm and a gap of 1mm was used to establish flow rates up to 4  $\text{s}^{-1}$  [8]. The use of an outer rotating cup, a sealed cell, and conical geometry in the cell base [13] provided a wider range of accessible shear rates for the neutron scattering measurements. Both the SANS and SAXS data were corrected and normalised using standard procedures [12,14].

Conductivity measurements were made using a customised cell, and have been described in detail elsewhere [1]. Light scattering measurements were made in the neutron Couette flow cell; which was illuminated with white light, viewed through crossed polarizers, and recorded using a digital camera.

## Inhomogeneous Distributions

The shear-thickening transition observed in the rheological response of the concentrated 2HT

dispersions (Fig. 1) was characterised by SANS and conductivity measurements to produce a 'shear diagram' (Fig. 2). This shows the shear-rate dependence of the transition from the aligned lamellar phase to multi-lamellar vesicles.

The 'shear diagram' is the out-of-equilibrium equivalent of an equilibrium phase diagram, and has been discussed in detail elsewhere [1]. The SANS data, measured in both the radial (neutron beam incident normal to the flow-vorticity plane) and tangential (neutron beam incident normal to the gradient-vorticity plane) scattering geometries, for the aligned lamellar phase reveal an apparent inconsistency (Fig. 3).

The orientational order observed in Figure 3(b), measured in the tangential scattering geometry, is consistent with lamellae oriented in the flow-vorticity plane, as previously reported [6]. For such orientational order there should be little or no scattering when measured in the radial scattering geometry, and this has been previously observed for other lamellar phase dispersions [6]. The pronounced scattering observed here (Fig. 3(a)), when measured in the radial scattering geometry, is, however, consistent with lamellae ordered in the flow-shear gradient plane. This has been observed previously in the lamellar phase of monohexadecyl hexaethylene glycol, C16E6 [6], and sodium dodecyl sulphate, SDS / dodecane / pentanol [7,8] at higher shear rates. However, in such cases the same scattering was observed in both the radial and tangential scattering geometries, and this is not the case for the 2HT data presented here in Figure 3. At intermediate shear rates, scattering in both the vorticity and shear flow directions has also been observed in C16E6 [6], and SDS / dodecane / pentanol [7], and was attributed to a bi-modal distribution of orientations. Subsequent measurements on SDS / dodecane / pentanol [8] showed that this was consistent with an inhomogeneous distribution across the Couette flow cell gap.

The results reported here for 2HT are not entirely consistent with those reported by Berghausen *et al.* [8], and require a slightly different explanation. On the basis of the SANS data the implication is that the lamellae close to the outer surface of the Couette flow cell gap are aligned parallel to the flow-vorticity plane, and that there is a distribution of orientations across the gap. The scattering in the tangential

Shear Stress,  $\sigma$  / Pa

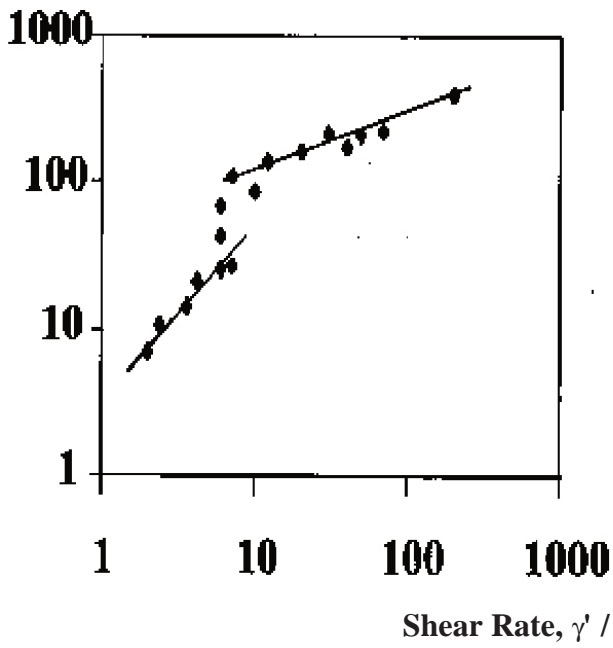


Figure 1. Shear stress,  $\sigma$ , as a function of shear rate,  $\gamma'$ , for 45 wt % 2HT.

Shear Rate,  $\gamma' / s^{-1}$

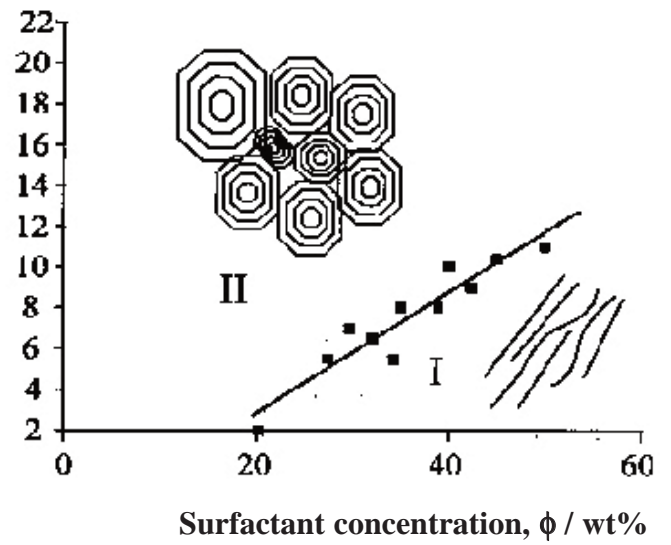
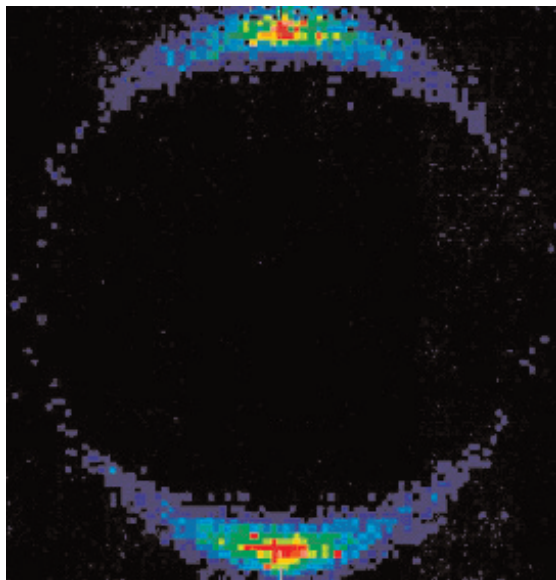
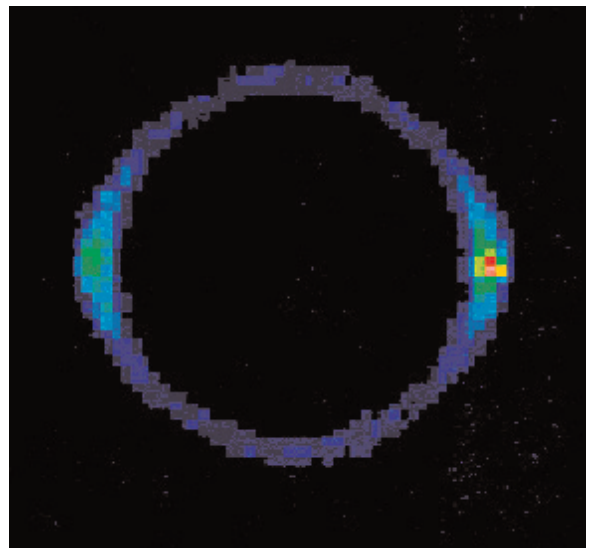


Figure 2. 'Shear diagram' for 2HT, shear rate,  $\gamma'$ , as a function of surfactant concentration,  $\phi$ , (in wt %), showing the stability regions of the two time invariant states as a function of shear rate



(a)



(b)

Figure 3. Two-dimensional SANS pattern for 45 wt% 2HT at a shear rate of  $6 \text{ sec}^{-1}$ , (a) radial scattering geometry, (b) tangential scattering geometry

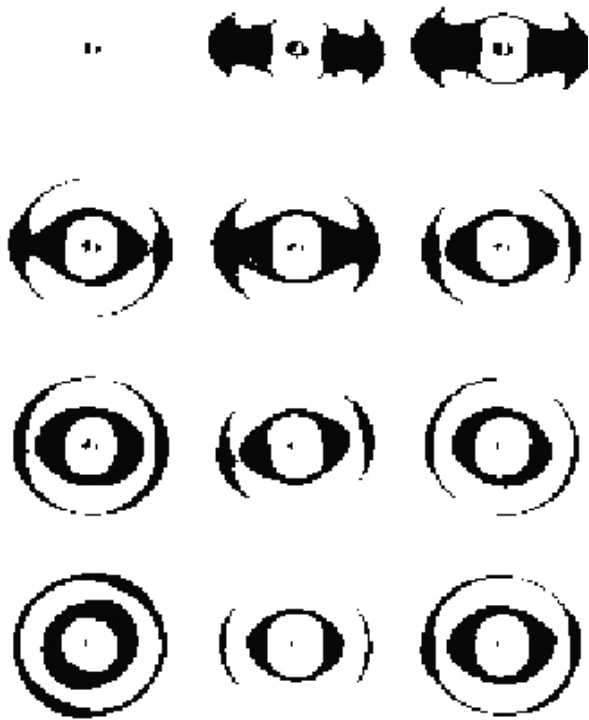


**Figure 4.** Two-dimensional SAXS scattering patterns for 45 wt% 2HT at a shear rate of  $0.4 \text{ s}^{-1}$ , from the outer surface towards the centre in 0.1mm steps (starting from the top left hand corner and increasing row by row)

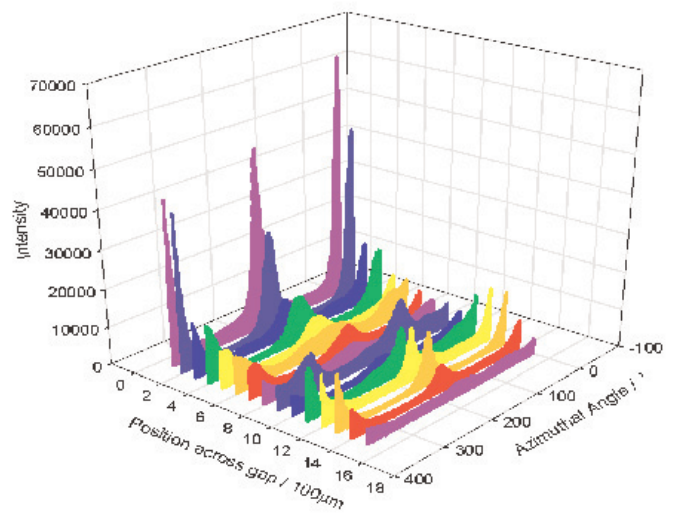
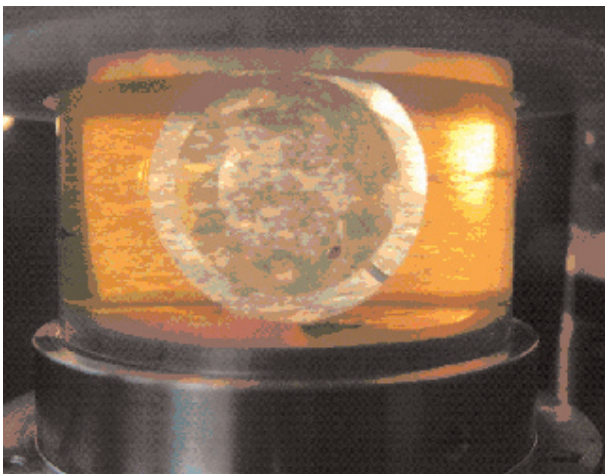
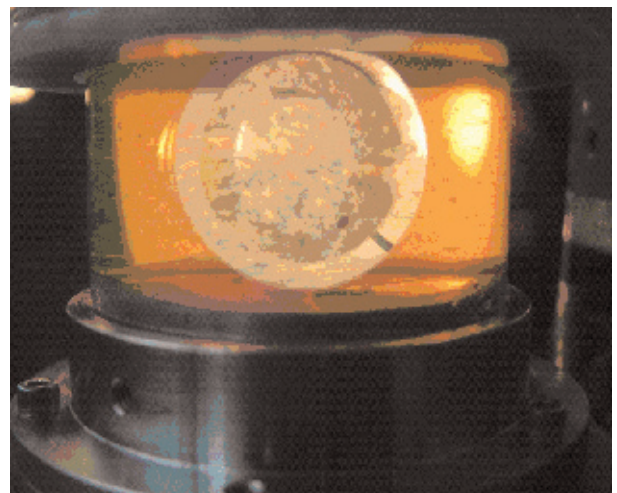


**Figure 5.** Scattered x-ray intensity as a function of azimuthal angle, from the outer surface towards the centre of the cell in 0.1mm steps, corresponding to the two-dimensional images in figure 4.



(a)



(b)

**Figure 6.** Polarised light scattering from 45 wt% 2HT at a shear rate of (a)  $8 \text{ s}^{-1}$ , (b)  $2 \text{ s}^{-1}$

geometry will be dominated by the fraction aligned close to the outer surface, whereas the greater neutron path length towards the cell centre will effectively attenuate the scattering from the inner regions of the gap. (Note: At 0.05 mm from the outer surface the mean path length is 4.4mm, whereas at 0.9mm it is 19.1mm. Assuming that a 1mm thick sample has a transmission  $\sim 0.8$ , then the change in mean transmission moving from 0.05 to 0.9 mm from the outer surface of the cell is  $\sim 40$ .) In the radial geometry there is no such preferential adsorption, and all regions of the gap will equally contribute to the observed scattering.

To confirm that the SANS scattering observed in the radial and tangential scattering geometries is consistent with an inhomogeneous distribution of orientations across the beam [14], as described in the experimental details section, two-dimensional SAXS scattering patterns are shown in Figure 4, for a series of positions at 0.1mm intervals across the Couette cell gap from the outer surface towards the inner surface.

Figure 5 shows the variation in scattered intensity as a function of azimuthal angle at a Q value corresponding to the second order Bragg peak arising from the ordered lamellar structure. There is a distribution of orientations across the flow cell gap. The lamellae closest to the outer surface are highly aligned in the flow-vorticity direction. There is a lower degree of orientational order further into the cell, and there are regions where the orientation is predominantly in the flow-shear gradient direction. The reduction in orientational order is partly due to averaging over the Couette cell curvature, but the changes in the direction of the orientational order are real. The distinct regions of orthogonal order raise the question of whether this distribution of orientational order is consistent with 'shear banding' [9,10].

'Shear banding' occurs in the proximity of a discontinuity in the stress-strain curve, and can be associated with a phase transition, with different micro-structures, with different orientational ordering, or with concentration changes (de-mixing). For both shear-thickening and shear-thinning systems, common strain 'banding' (in the vorticity direction) and common stress 'banding' (in the shear gradient direction) are possible. If the applied strain rate forces the system into the unstable part of the flow curve, then it can separate into regions (or

bands) with high and low strain rates, whilst maintaining the applied strain rate. The radial separation in common stress 'banding' imposes a uniform shear stress and different strain rates, whereas the axial separation in common strain 'banding' results in the same strain rate but different shear stresses.

It was not possible to make the SAXS measurements at a shear rate close to the discontinuity shown in Figure 1, and the rheology measurements are not sufficiently detailed at the lower shear rates to correlate the SAXS data measured at  $0.4 \text{ s}^{-1}$  directly with a specific rheological response. Further rheology measurements are required to confirm whether the micro-focus SAXS data are consistent with common stress 'banding'.

To explore the possibility of common stress 'banding' in this system, some polarised light scattering measurements were made in the region of the stress / strain discontinuity (Fig. 1) in the neutron Couette flow cell. The results are shown in Figure 6. There is a pronounced increase in the texture of the light scattering in the region of the rheological discontinuity. However, there is no marked development of macroscopic bands. The evolution of banding in the vorticity direction is controlled by 1-D diffusion, and is hence slow. Further measurements at longer incubation times (the measurements in Figure 6 were made after  $\sim 5$  to 10 minutes) will be made. The measurements will also be made at constant stress, rather than constant strain. Common stress and common strain 'banding' has been observed in related lamellar phase systems [15], and in worm-like or elongated micellar structures [16-18]. The measurements made so far for the 2HT system show a distribution of orientational order in the shear gradient direction, and demonstrate the possibility of shear 'banding'.

### Effects of temperature and co-surfactant

In the previous section we have highlighted some aspects of the effects of shear on concentrated surfactant dispersions, and the relationship between the micro-structure and the macroscopic rheological response. For the di-chain cationic surfactants, which are used extensively in a variety of formulations, temperature and the addition of a co-surfactant can have a profound effect on the micro-structure of these lamellar phase dispersions. The  $L_\alpha / L_\beta$  transition, the transition from an ordered

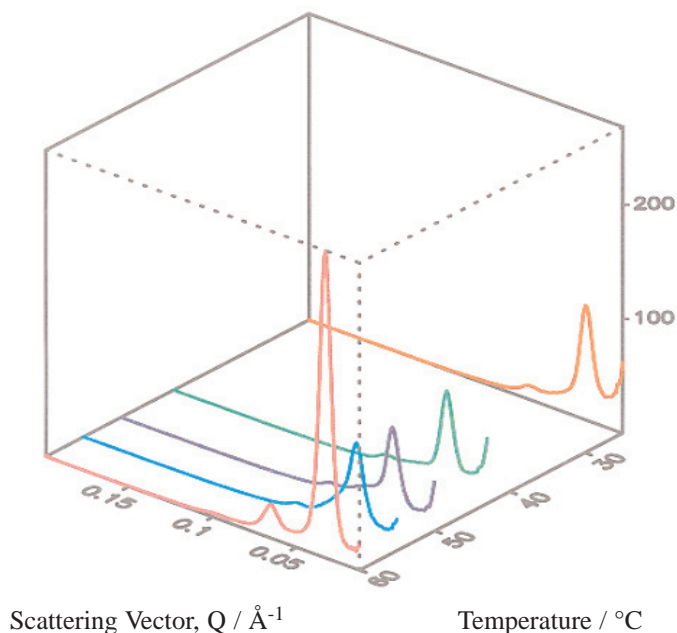


**Figure 7.** Scattered Intensity,  $I(Q)$ , as a function of temperature for 12 wt% HEQ / 4 wt % C12E12

'solid-like' phase to fluid bilayers, has a significant impact on the dispersion micro-structure. The addition of co-surfactants will modify (lower) that transition temperature. The non-ionic co-surfactant will adsorb to the edge of lamellar fragments, stabilise smaller fragments, and reduce the dispersion viscosity. We present here some preliminary SANS data on the effects of temperature and the composition of di-chain cationic / non-ionic surfactant mixtures, which complement and extend the results which highlight the role of shear.

A series of SANS measurements for a mixture of the di-chain cationic and non-ionic surfactants, 2,3-diheptadecyl ester ethoxy-n-propyl-1,1,1-trimethyl ammonium chloride, HEQ and dodecaethylene glycol monododecyl ether, C12E12, rich in the cationic surfactant and as a function of temperature are shown in Figure 7. At all temperatures the data are consistent with lamellar fragments. Increasing the temperature above the  $L_\alpha / L_\beta$  transition temperature ( $\sim 50^\circ\text{C}$ ) results in a more ordered lamellar structure. Applying modest shear ( $\leq 10 \text{ s}^{-1}$ ) produces pronounced anisotropy (see Fig. 8). The scattering at  $55^\circ\text{C}$  shows 4 to 5 orders of diffraction, and is consistent with a highly ordered and oriented lamellar phase. Reducing the cationic / non-ionic composition of the dispersion results in a rather different structural response with increasing temperature (see Fig. 9), and evolution of a different

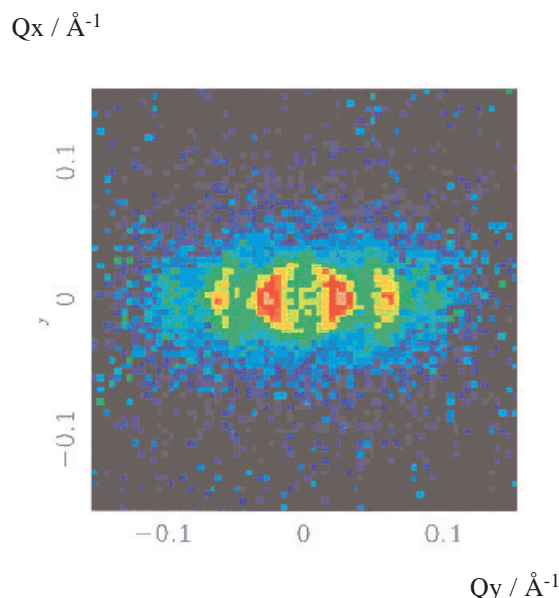


**Figure 8.** 2-D Intensity contour pattern for 12 wt % HEQ / 4 wt % C12E12 at  $55^\circ\text{C}$  and a shear rate of  $10 \text{ s}^{-1}$ .

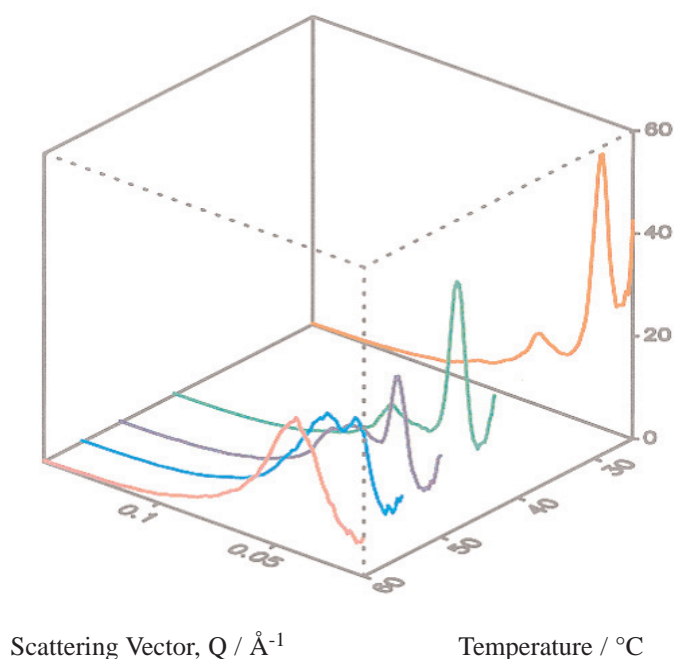


**Figure 9.** Scattered Intensity,  $I(Q)$ , as a function of temperature for 4 wt% HEQ / 4 wt% C12E12

sequence of micro-structures.

With increasing temperature the scattering evolves from that corresponding to lamellar fragments to mixed surfactant micelles. At intermediate temperatures micelles and lamellar fragments co-exist. Increasing the temperature has induced the formation of mixed micelles from the lamellar dispersion, such that above the  $L_\alpha / L_\beta$  transition temperature the solution is entirely micellar. Further measurements exploring more completely the phase

behaviour, micro-structure and rheology of such mixtures are now underway.

## Summary

We have used a combination of scattering techniques and rheological measurements to understand the micro-structure of complex concentrated di-chain cationic lamellar phase dispersions, and the effects of shear, temperature and the addition of co-surfactants on such dispersions. We have provided evidence of the inhomogeneities in orientational order arising in Couette flow, and we have discussed the data in relationship to the possibilities of 'shear banding'. We have presented preliminary results showing the evolution of order and structure with temperature and with the addition of a co-surfactant. The data show an increase in lamellar order with temperature and the development of mixed micelles.

## References

- [1] Soubiran, L., Staples, E., Tucker, I. & Penfold, J. (2001) Effects of shear on the lamellar phase of a di-chain cationic surfactant. *Langmuir* **17**, 7988-7994.
- [2] Olmsted, P.D. (1999) Two-state shear diagram for complex fluids in shear flow. *Europhys Lett* **48**, 339-345.
- [3] Berret, J.F., Roux, D.C., Porte, G. & Lindner, P. (1994) Shear-induced isotropic to nematic transition in equilibrium polymers. *Europhys Lett* **25**, 521-
- [4] Berret, J.F., Gamez-Corrales, R., Serero, Y., Molino, F. & Lindner, P. (2001) Shear induced micellar growth in dilute surfactant solutions. *Europhys Lett*. **54**, 605-611.
- [5] Diat, O., Roux, D.C. & Nallet, F. (1993) Effect of shear on lyotropic lamellar phase. *J. Phys. II* **3**, 1427-1452: (1995) Layering effect in a sheared lyotropic lamellar phase. *Phys. Rev. E* **51**, 3296-3299.
- [6] Penfold, J., Staples, E., Tucker, I., Tiddy, G.J.T. & Khan Lodi, A. (1997) Shear induced transformation in the lamellar phase of C16E6. *J. Phys. Chem. B* **101**, 66-72: (1997) Shear induced structures in concentrated micellar phases. *J. Appl. Cryst.* **30**, 744-749.
- [7] Zipfel, J., Berghausen, J., Lindner, P. & Richtering, W. (1999) Influence of shear on lyotropic lamellar phases with different membrane defects. *J. Phys. Chem. B* **103**, 2841-2849.
- [8] Berghausen, J., Zipfel, J., Diat, O., Narayanan, T. & Richtering, W. (2002) Lamellar phases under shear: variation of the layer orientation across the Couette gap. *PCCP* **2**, 3623-3626.
- [9] Olmsted, P.D. & Lu, C.Y.D. (1997) Coexistence and phase separation in sheared complex fluids. *Phys. Rev. E* **56**, R55-R58; (1999) Phase coexistence of complex fluids in shear flow. *Faraday Disc.* **112**, 183-194.
- [10] Goveas, J.L. & Olmsted, P.D. (2001) A minimal model for vorticity and gradient banding in complex fluids. *Eur. Phys. J. E* **6**, 79-89.
- [11] Partal, P., Kowalski, A.J., Machin, P., Kiratzis, N., Berni, M.G. & Lawrence, C.J. (2001) Rheology and microstructure transition in the lamellar phase of a cationic surfactant.

*Langmuir* **17**, 1331-1337.

- [12] Heenan, R.K., King, S.M. & Penfold, J. (1997) SANS at a pulsed neutron source. Present and future prospects. *J Appl Cryst* **30**, 1140-1147.
- [13] Cummins, P.G., Staples, E., Millen, B. & Penfold, J. (1990) A Couette flow cell for small-angle scattering studies. *Meas. Sci. Technol.* **1**, 179-183.
- [14] Engstrom, P., Fielder, S. & Riekel, C. (1995) Microdiffraction instrumentation and experiments with the microfocus beamline at the ESRF. *Rev. Sci. Instrum.* **66**, 1348-1350.
- [15] Bonn, D., Meunier, J., (1998) Bi-stability in non-Newtonian flow: rheology of lyotropic liquid crystals. *Phys. Rev. B* **58**, 2115-2118.
- [16] Lerouge, S., Decruppe, J.P. & Berret, J.F. (2000) Correlations between rheology and optical properties of a micellar solution under shear banding flow. *Langmuir* **16**, 6464-6474.
- [17] Fischer, E. & Callaghan, P.T. (2001) Shear banding and the isotropic to nematic transition in worm-like micelles. *Phys. Rev. E* **64**, 011501-011510.
- [18] Decruppe, J.P., Cressely, R., Makhloufi, R. & Cappelaere, E. (1995) Flow birefringence experiments showing a shear banding structure in a CTAB solution. *Coll. Polym. Sci.* **273**, 346-351.